International Research Journal of Engineering and Technology (IRJET) e-ISSN: 2395-0056
Volume: 09 Issue: 10 | Oct 2022 www.irjet.net p-ISSN: 2395-0072

COMPUTATIONAL FLUID DYNAMIC ANALYSIS OF NACA 0006 AEROFOIL AT DIFFERENT PARAMETERS WITH REGRESSION ANALYSIS

***Pavan Chaitanya*[1,a], *Dr. G. Srinivas Sharma*[2,b]**

[1]*UG scholar, Department of Mechanical Engineering, India*
[2]*Associate Professor, Department of Automobile Engineering, India*
Maturi Venkata Subba Rao (MVSR) Engineering College, Telangana, India
Email: [a]pavanchaitanya.01@gmail.com, [b]hod_auto@mvsrec.edu.in

---

ABSTRACT

This study investigates the factors influencing the performance of an aerofoil that is intended to be used in a flight system. Wind speed and angle of attack parameters are crucial for perfect flight. The inlet flow velocity along the surface of the aerofoil geometry is varied from 5 to 25m/s with 5m/s interval. Here, a numerical investigation using ANSYS Fluent, of two-dimensional incompressible flow over a NACA 0006 aerofoil is analysed at various mach numbers by varying angle of attack. The purpose of this research is to study the flow pattern over an aerofoil using CFD. Variation of pressure and velocity counters are plotted. The variations in coefficient of lift and coefficient of drag with respect to various angles of attack is analysed.

Key Words- *NACA 0006 aerofoil, coefficient of lift and drag, angle of attack, pressure and velocity counters*

1. INTRODUCTION

The method of simulating a fluid flow mathematically related to a physical event and solving it numerically utilizing computational power is known as computational fluid dynamics (CFD). It is undertaken to examine fluid flow in relation to its physical characteristics such as velocity, pressure, density, and viscosity. Those features must be taken into account simultaneously in order to practically develop an precise solution for a physical phenomenon connected to fluid flow.

To analyse fluid flow, a CFD software tool employs a numerical method and mathematical model. The pressure distribution over the aerofoil surface often affects both the lift force and the pitching moment. The distribution of friction and pressure along the surface affects the drag force.

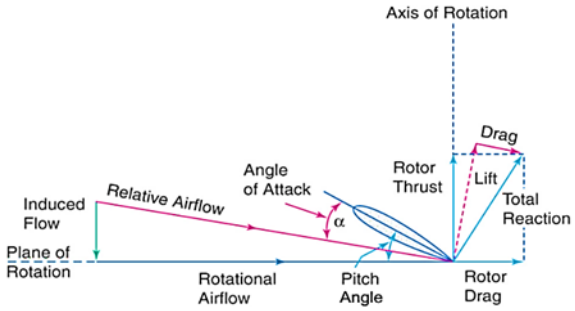

Fig.1. Basic aerodynamic forces acting on an aerofoil

Dimensionless coefficients are taken into account in comparisons and assessments due to the diverse shapes and sizes of the aerofoil created for distinct purposes. The result of the wing's motion in free stream is a lift force that is perpendicular to its motion and larger than the downward gravity force on the wing, keeping the aircraft in the air. The effective wing area that faces the airflow directly affects drag, as does the shape of the wing. The angle of attack between the wing's direction of flight and the chord line of the blade influences the lift and drag.

The following two-dimensional calculations were made to account for C_L equation (1) and C_D equation (2) in the performance assessment of the airfoils. L (the L lift force), D (the D drag force), V (the V wind speed), ρ (the ρ fluid density), and S are additional factors in the equation (the S aerofoil surface area). Following the dimensionless calculation of these factors, the CL/CD ratio can be practically applied for performance comparisons.

$$C_L = \frac{L}{(1/2)\rho V^2 S} \text{ ----------(1)}$$

$$C_D = \frac{D}{(1/2)\rho V^2 S} \text{ ----------(2)}$$

1.1. Material and method

The surface curve coordinates that define the typical NACA 0006 blade geometry were imported to create the blade section geometry. The properties of the

aerodynamic system have been examined using computational fluid dynamics (CFD).

1.2 Blade Sections and Aerodynamic Properties

NACA aerofoils are those that have been standardised by the National Advisory Committee for Aeronautics (NACA). Their geometries are defined by a series of digits. NACA aerofoils come in four-digit, five-digit, one-series, and other variations. In this study, one of the four-digit NACA profiles, NACA 0006, is selected and tested in the analysis. The "00" first digits of the wing indicate that it lacks camber and has a symmetrical profile. The thickness to chord length ratio is represented by the other digits "06." The thickness of the wing is 6% [1], [2]. Its form is encoded in an equation. [3] is the symmetrical four-digit NACA aerofoil.

$$y_t = 5.t.c.\left[0.2969.\sqrt{\frac{x}{c}} + (-0.126).\frac{x}{c} + (-0.3516).\left(\frac{x}{c}\right)^2 + 0.2843.\left(\frac{x}{c}\right)^3 + (-0.1015).\left(\frac{x}{c}\right)^4\right] \text{------(3)}$$

Where:

"yt " is the half-thickness of the aerofoil

"t" is the maximum thickness

"c" is the chord length

"x" is the position

2. LITERATURE REVIEW

Shubham [4] has researched on the effect of lift and drag using typical root aerofoil section of Boeing 737 aircraft wing model for various angles ranging from -4° to 22° using CFD and also analysed adverse parameters of stall angle and yaw for test aerofoil.

B S Gawali and Pravin Mane [5] An experimental and Computational analysis (CFD) was performed at an air flow rate of 15m/s over an aerofoil at different angles of attack ranging from 0° to 20°. The findings of the study demonstrated the pressure distribution over the aerofoil as well as the action of lift force on the aerofoil.

Rajat, Kiran, Vipul, Pritam [6] analysed the aerofoil over 2D subsonic flow at a varying angle of attack that is operating at Reynolds's number were obtained and concluded that flow has occured separation away from the rear edge that reduces the generated lift.

Karna, Saumil, Utsav, Prof. Ankit analytically analysed the 2D subsonic flow at varying angle of attack working at a Re of 3×E+06 on NACA 0012 aerofoil[7].

3. GEOMETRY AND MODELLING

The XY plane has been chosen to build the aerofoil and fluid domain models. The Cartesian coordinates of NACA 0006 aerofoil have been imported from the UIUC aerofoil database[8]. The aerofoil has approximately 1 m of chord length. The C-type fluid domain of 10C has been constructed in the Design Modeller of ANSYS workbench. In order to have greater control over the mesh generation, the domain has been sliced into four surfaces by drawing a horizontal line through the aerofoil and vertical line at the straggling edge of the aerofoil. The projection tool has been selected to project the four surfaces onto the fluid domain.

Far Field mesh is created using the Design Modeller with dimensions of 12.5m in radius and length. The curvature part is taken as inlet and the sides as walls, end line as outlet.

Airfoil Parameters

Chord (mm) **–100**

Radius (mm) – **0**

Origin (%) – **0**

Pitch (°) **– 0**

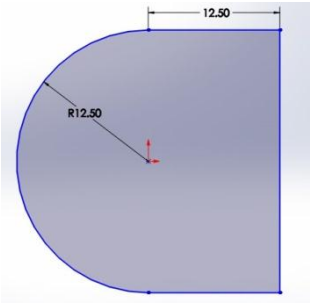

Fig.2. FarField Mesh Sketch(in m)

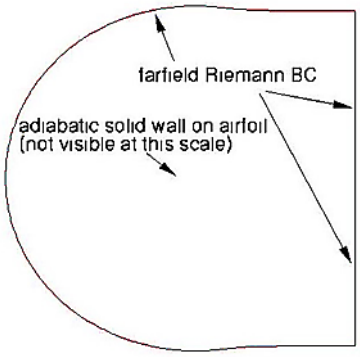

Fig.3. FarField BC description

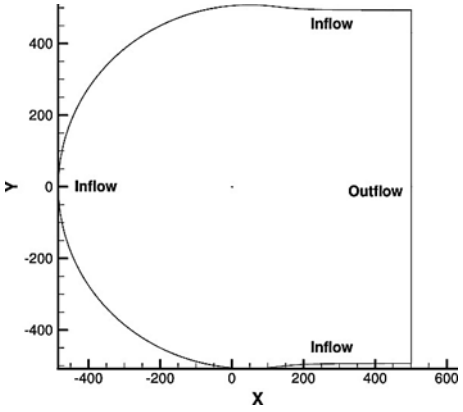

Fig.4. FarField BC flow description

4. MESH GENERATION & BOUNDARY CONDITIONS

In the finite element method, the fluid domain discretized into smaller elements based on a specific shape. The Triangular structured mesh has been applied in the fluid domain as it can provide better accuracy compared to the unstructured mesh.

The aerofoil has been initialized as no-slip and treated as wall boundary as the flow energy has been lost into dissipation and brought to rest as it approached the surface. The flow whose density remained unchanged is defined as the incompressible flow is defined as the flow that has constant density and Mach number M<=0.3. Therefore, the constant air density has been set as the material of the fluid. The velocity inlet has been set from 5 - 25 m/s, which was equivalent to a Mach number of 0.01 - 0.07.

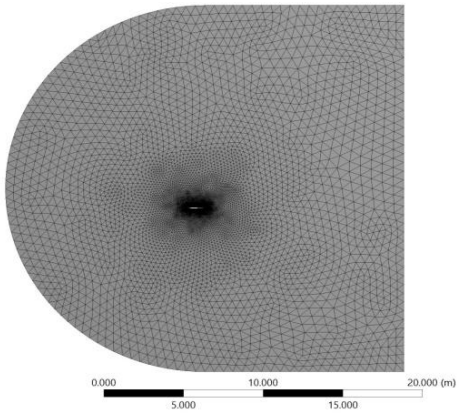

Fig.5. FarField Mesh

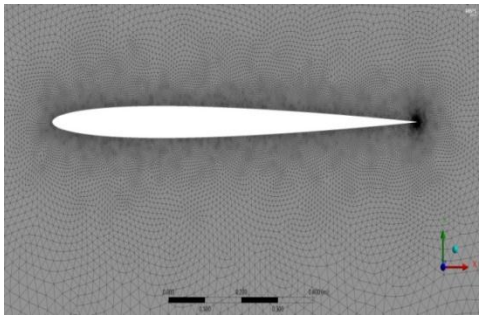

Fig.6. Mesh around Airfoil

Triangular Mesh with suitable Refinements and Sizing was used for generating mesh to improve the quality of the output. Inflation was established around the aerofoil curve.

For turbulent flow conditions, to simulate characteristics of mean flow the most commonly used model in CFD is the k-epsilon (k- ϵ) turbulence model suitable.

It is a model that uses two transport equations to provide a general elucidation of turbulence. A new generation of equation for turbulent viscosity is included in the realisable k- ϵ model.

Compressibility has an impact on turbulence at high Mach numbers through a process known as "dilatation dissipation," which is typically overlooked in the modelling of incompressible flows .The observed drop in spreading rate with rising Mach number for compressible mixing and other free shear layers cannot be predicted without taking into account dilatation dissipation.[9]

$$Y_M = 2\rho\epsilon M_t^2 \text{-------(4)}$$

Where, M_t is the turbulent Mach number, defined as

$$M_t = \sqrt{\frac{k}{a^2}} \text{--------(5)}$$

Where, a ($\equiv \sqrt{\gamma RT}$) is the speed of sound.

This compressibility modification always applies when the ideal gas law is applied in its compressible form.

Transport Equations for the Realizable

$k-\epsilon$ Model

The modelled transport equations for **k** and ϵ in the realizable $k-\epsilon$ model are

$$\frac{\partial}{\partial t}(\rho k) + \frac{\partial}{\partial x_j}(\rho k u_j) = \frac{\partial}{\partial x_j}\left[\left(\mu + \frac{\mu_t}{\sigma_k}\right)\frac{\partial k}{\partial x_j}\right] + G_k + G_b - \rho\epsilon - Y_M + S_k \text{--------(6)}$$

$$\frac{\partial}{\partial t}(\rho\epsilon) + \frac{\partial}{\partial x_j}(\rho\epsilon u_j) = \frac{\partial}{\partial x_j}\left[\left(\mu + \frac{\mu_t}{\sigma_\epsilon}\right)\frac{\partial \epsilon}{\partial x_j}\right] - C_{2\epsilon\rho}\frac{\epsilon^2}{k} + C_{1\epsilon}\frac{\epsilon}{k}(G_k + C_{3\epsilon}G_b) + S_\epsilon \text{--------(7)}$$

$$C_1 = \max\left[0.43, \frac{\eta}{\eta+5}\right], \eta = S\frac{k}{\epsilon}, S = \sqrt{2S_{ij}S_{ij}}$$

Equation 4 describes the generation of turbulence kinetic energy due to the mean velocity gradients denoted as G_k. Equation 5 describes the generation of turbulence kinetic energy due to buoyancy signified as G_b. For ϵ and k, the turbulent Prandtl numbers are σ_ϵ and σ_k. Some user-defined source terms are S_ϵ and S_k and constants are $C_{1\epsilon}$ and $C_{2\epsilon}$.[9]

MODEL SETUP

K-Epsilon (2 eqn)

C2 – Epsilon - 1.9

TKE Prandtl Number - 1

TDR Prandtl Number - 1.2

K-Epsilon Model - Realizable

Near - Wall Treatment

Standard Wall Functions

Viscosity (kg/m-s) - 1.7894e-05

Temperature – 300k

5. RESULTS AND DISCUSSIONS

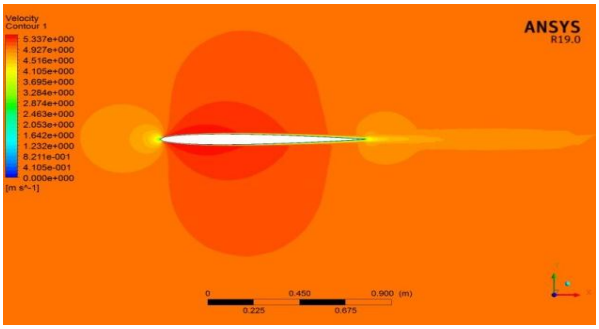

Fig.7. Velocity Contour at 0° AoA

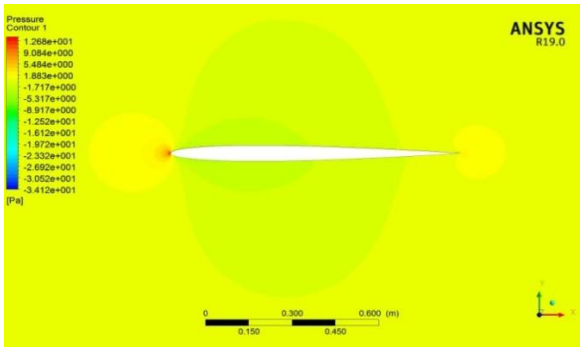

Fig.8. Pressure Contour at 0° AoA

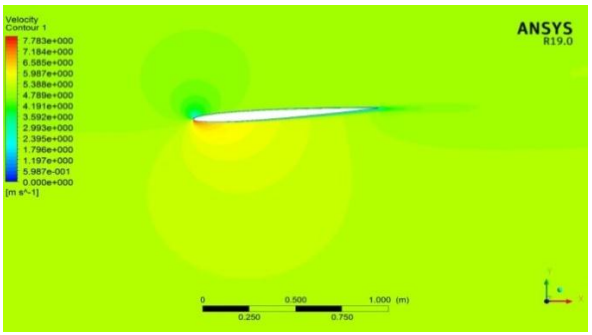

Fig.9. Velocity Contour at -4° AoA

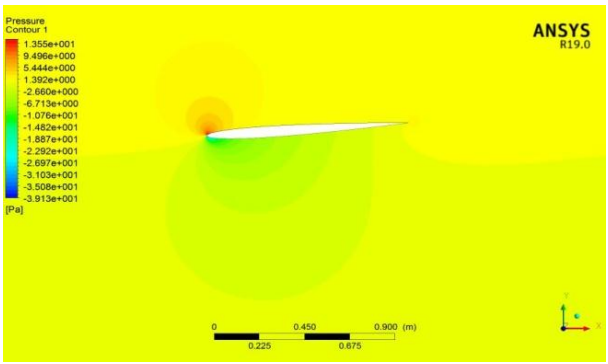

Fig.10. Pressure Contour at -4° AoA

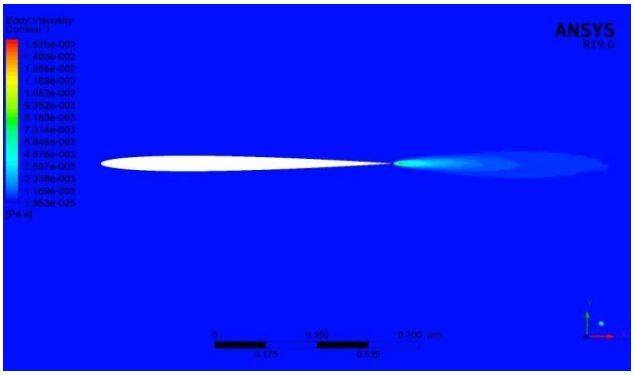

Fig.11. Eddy Viscosity Contour

Table 1. Depicting Min/ Max values

Contour	Min value	Max value
Density (kgm^{-3})	1.225	1.225
Eddy Viscosity (Pas)	1.9527e-25	0.0155868
Pressure (Pa)	-34.1172	13.8837
Pressure.Gradient ($kgm^{-2}s^{-2}$)	3.28287e-05	5.63732e+06
Turbulence Eddy Dissipation (m^2s^{-3})	9.30091e-07	1.85124e+08
Turbulence Kinetic Energy ($m^{-2}s^{-2}$)	1e-14	89.7405
Velocity (m/s)	0	5.47391
Wall Shear (Pa)	0.000235352	9.62613

Table 2. Coefficient of lift and drag for varying angle of attack(AoA) at Inlet velocity of 5m/s

Angle of Attack (°)	Coefficient of Lift (C_l)	Coefficient of Drag (C_d)	C_l/C_d
-4	-0.41038	0.015111	-27.15769969
-3	-0.29938	0.013874	-21.57849214
-2	-0.17504	0.013087	-13.37510507
-1	-0.091045	0.012463	-7.305223461
0	-0.0073066	0.01644	-0.444440389
1	0.11808	0.012196	9.681862906
2	0.10653	0.012509	8.516268287
3	0.24542	0.014442	16.99349121
4	0.40821	0.016606	24.58207877
5	0.45399	0.017987	25.23989548

Table 3. Coefficient of lift and drag for varying angle of attack(AoA) at Inlet velocity of 25m/s

Angle of Attack (°)	Coefficient of Lift (C_l)	Coefficient of Drag (C_d)	C_l/C_d
-4	-0.37186	0.012621	-29.46359243
-3	-0.27619	0.011291	-24.46107519
-2	-0.10329	0.017134	-6.028364655
-1	-0.061246	0.0095662	-6.402333215
0	-0.0034407	0.0091379	-0.376530713
1	0.20387	0.0085699	23.78907572
2	0.08704	0.010045	8.665007466
3	0.2037	0.011288	18.04571226
4	0.42534	0.014461	29.41290367
5	0.51777	0.013938	37.14808437

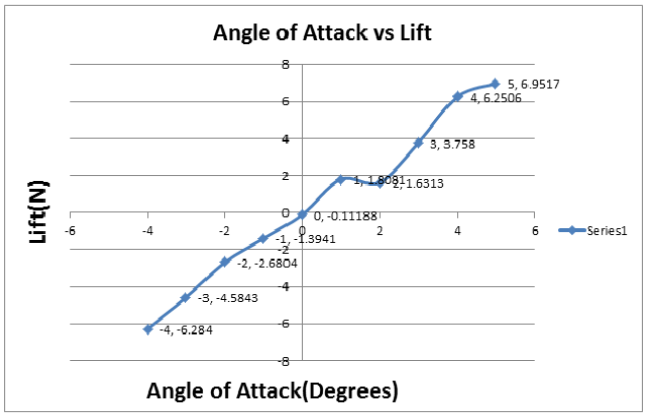

Fig.12. Graph AOA vs Lift at 5m/s

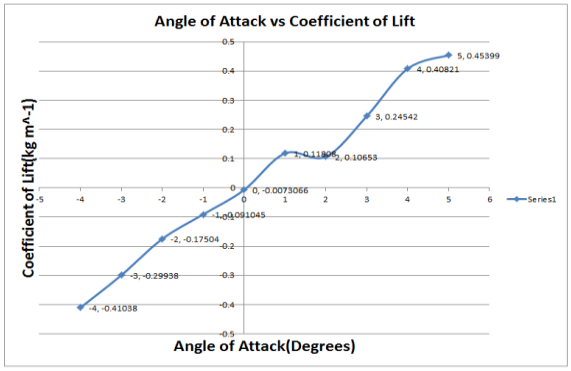

Fig.13. AOA vs Coefficient of Lift at 5m/s

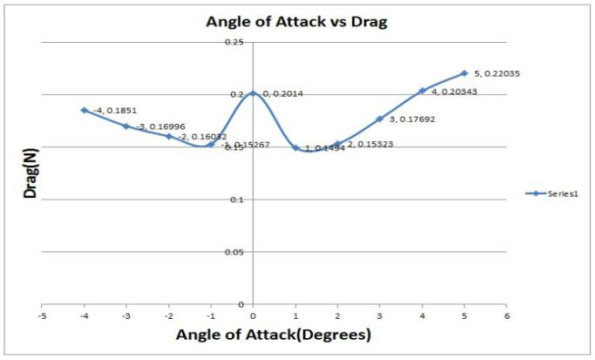

Fig.14. AOA vs Drag at 5m/s

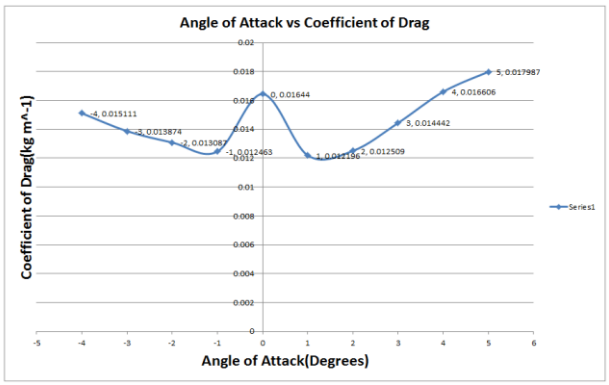

Fig.15. AOA vs Coefficient of Drag at 5m/s

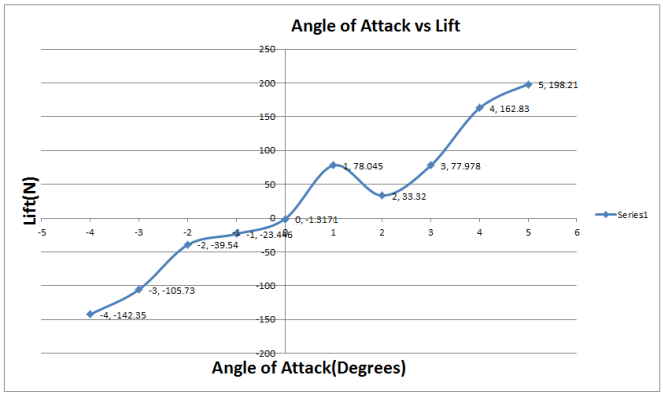

Fig.16. AOA vs Lift at 25m/s

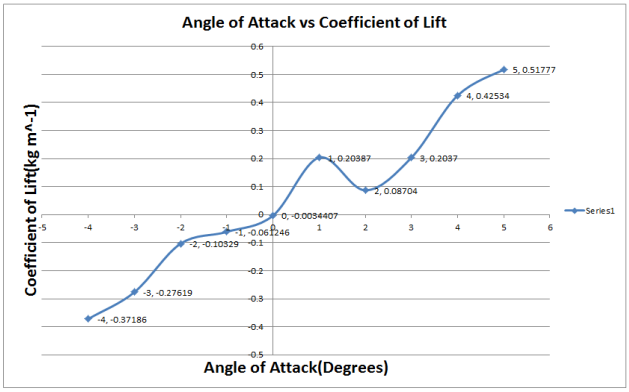

Fig.17. AOA vs Coefficient of Lift at 25m/s

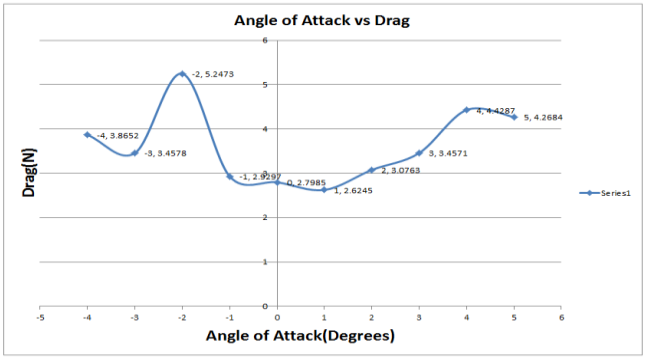

Fig.18. AOA vs Drag at 25m/s

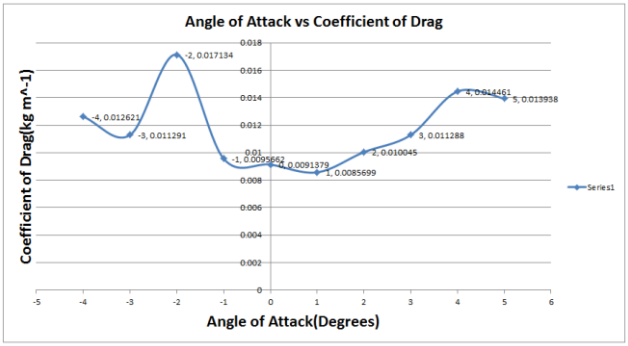

Fig.19. AOA vs Coefficient of Drag at 25m/s

6. REGRESSION ANALYSIS

A simple technique for determining the functional relationship between variables and the influence of variables on response is known as regression analysis. This analysis is carried out using the Mini Tab software.

Using regression analysis as equation 8-10, a mathematical model is created. The developed equation is based on simulated data, with the response represented by the ratio of coefficient of lift (C_l) to coefficient of drag (C_d) and the dependent variable represented by the angle of attack.

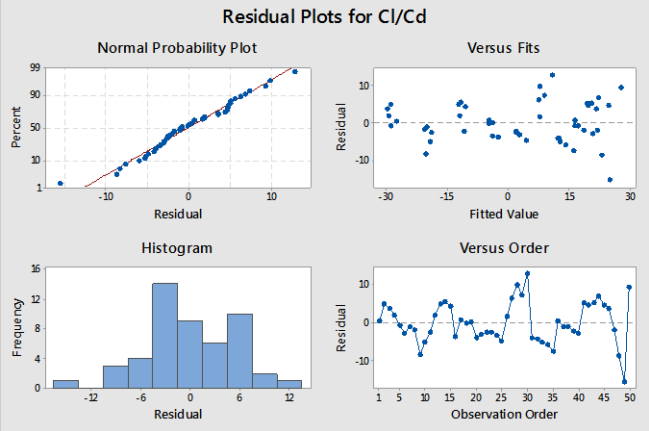

Fig.20. Residual plots for Cl/Cd

Regression Equation

Cl/Cd = 3.83 + 5.670 × AoA - 0.337 × Inlet Velocity + 0.0407 × AoA × Inlet Velocity - 0.409 AoA × AoA + 0.0146 × Inlet Velocity × Inlet Velocity ---------(8)

Model Summary

S = 5.66958

R-sq = 91.25%

R-sq(adj) = 90.26%

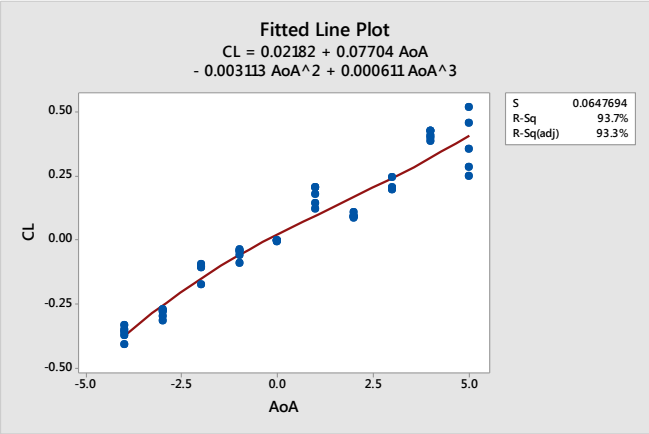

Fig.21. Coefficient of lift (C_l) data fitted to mathematical curve

Regression Equation

Cl = 0.02182 + 0.07704 × AoA - 0.00313× AoA^2 + 0.000611 × AoA^3 ----------(9)

Model Summary

S = 0.0647694

R-sq = 93.7%

R-sq(adj) = 93.3%

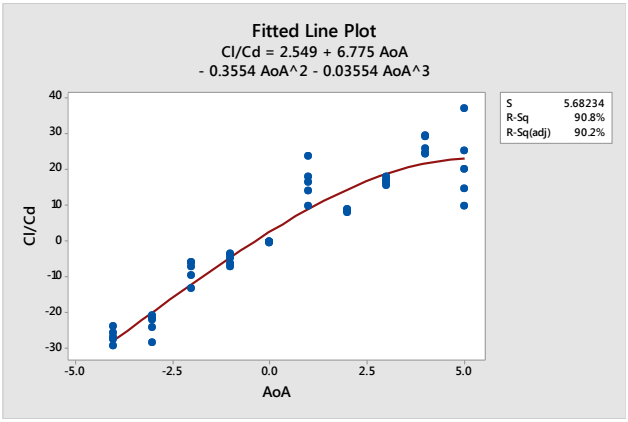

Fig.22. Coefficient of lift (C_l) to Coefficient of drag (C_d) Cl/Cd data fitted to mathematical curve

Regression Equation

Cl/Cd = 2.549 + 6.775 × AoA - 0.3554 × AoA^2+ 0.03554 × AoA^3 ----------(10)

Model Summary

S = 5.68234

R-sq = 90.8%

R-sq(adj) = 90.2%

7. CONCLUSIONS

With increase in angle of attack it is observed that lift has increased and peaked at 5°, whereas at 0° the drag is greater than lift which is not preferred in aircrafts as the main aim is to reduce the drag. 1° AoA is preferred over 2° as the lift produced is slightly greater, at negative AoA of -2° drag is peaked. These results are analysed with the standard NACA 0006 aerofoil. The aerofoil is best suitable for higher angle of attack.

At higher AoA better lift can be obtained by using this aerofoil so, the fuel efficiency will be improved by about 8%. The simulated value of the coefficient of lift is in good fit and with high accuracy to the mathematical model equation. This aerofoil is well pereferred at 5° AoA as drag is less, where the flight will emit less pollution and can be considered green flight.

REFERENCES

[1] "NACA Airfoils | NASA," 2017. https://www.nasa.gov/image-feature/langley/100/nacaairfoils (accessed Jan. 19, 2021).

[2] Jacobs J. N., Ward K. E., and Careas R. M., "The Characteristics of 78 Related Airfoil Sections Sections From Tests In The Variable-Density Wind Tunnel," National Advisory Commitee for Aeronautics, (1935).

[3] Anderson J. D., Fundamentals of Aerodynamics SI, McGraw-Hill, 1984(3), (2011).

[4] Shubham Prakash Rawool , "CFD analysis of boeing-737 3d aerofoil and adverse yaw on the aerofoil", , IJRET: International Journal of Research in Engineering and Technology , Vol 6, Issue 6, (2017), 2321-7308.

[5] Chandrakant Sagat, Pravin Mane and B S Gawali, Experimental and CFD analysis of airfoil at low Reynolds number, International Journal of Mechanical Engineering and Robotics Research, ISSN 2278 – 0149 Vol. 1, No. 3, October 2012

[6] Rajat Veer, Kiran Shinde, Vipul Gaikwad, Pritam Sonawane , "Study and Analyse Airfoil Section using CFD", International Journal of Engineering Research & Technology (IJERT), Vol. 6 Issue 09, (2017) 2278-0181.

[7] Karna S. Patel, Saumil B. Patel, Utsav B. Patel, Prof. Ankit P. Ahuja, "CFD Analysis of an Aerofoil", International Journal of Engineering Research Volume No.3, Issue No.3, (2014) 2319-6890.

[8] "Airfoil Tools." http://airfoiltools.com/ (accessed Feb. 04, 2021).

[9]Ansys Inc., "Ansys Fluent 12.0/12.1 Documentation" Ansys Inc., (12.0)